The Meteoritical Society

Meteoritics & Planetary Science 42, Nr 7/8, 1183–1195 (2007)
Abstract available online at http://meteoritics.org

^{26}Al-^{26}Mg systematics of Ca-Al-rich inclusions, amoeboid olivine aggregates, and chondrules from the ungrouped carbonaceous chondrite Acfer 094

Naoji SUGIURA[1*] and Alexander N. KROT[2]

[1]Department of Earth and Planetary Science, University of Tokyo, Tokyo, Japan
[2]Hawai'i Institute of Geophysics and Planetary Science, School of Ocean, Earth Sciences and Technology, University of Hawai'i at Manoa, Honolulu, Hawai'i 96822, USA
[*]Corresponding author. E-mail: sugiura@eps.s.u-tokyo.ac.jp

(Received 29 September 2006; revision accepted 02 March 2007)

Abstract–We report in situ magnesium isotope measurements of 7 porphyritic magnesium-rich (type I) chondrules, 1 aluminum-rich chondrule, and 16 refractory inclusions (14 Ca-Al-rich inclusions [CAIs] and 2 amoeboid olivine aggregates [AOAs]) from the ungrouped carbonaceous chondrite Acfer 094 using a Cameca IMS 6f ion microprobe. Both AOAs and 9 CAIs show radiogenic ^{26}Mg excesses corresponding to initial ^{26}Al/^{27}Al ratios between ~5×10^{-5} and ~7×10^{-5}, suggesting that formation of the Acfer 094 CAIs may have lasted for ~300,000 years. Four CAIs show no evidence for radiogenic ^{26}Mg; three of these inclusions (a corundum-rich, a grossite-rich, and a pyroxene-hibonite spherule CAI) are very refractory objects and show deficits in ^{26}Mg, suggesting that they probably never contained ^{26}Al. The fourth object without evidence for radiogenic ^{26}Mg is an anorthite-rich, igneous (type C) CAI that could have experienced late-stage melting that reset its Al-Mg systematics. Significant excesses in ^{26}Mg were observed in two chondrules. The inferred ^{26}Al/^{27}Al ratios in these two chondrules are $(10.3 \pm 7.4) \times 10^{-6}$ and $(6.0 \pm 3.8) \times 10^{-6}$ (errors are 2σ), suggesting formation $1.6^{+1.2}_{-0.6}$ and $2.2^{+0.4}_{-0.3}$ Myr after CAIs with the canonical ^{26}Al/^{27}Al ratio of 5×10^{-5}. These age differences are consistent with the inferred age differences between CAIs and chondrules in primitive ordinary (LL3.0–LL3.1) and carbonaceous (CO3.0) chondrites.

INTRODUCTION

In spite of more than thirty years of study of ^{26}Al-^{26}Mg systematics in chondritic meteorites, which has clearly shown the presence of live ^{26}Al in refractory inclusions (Ca-Al-rich inclusions [CAIs], amoeboid olivine aggregates [AOAs]), and chondrules (e.g., Lee et al. 1976; MacPherson et al. 1995; Kita et al. 2000, 2005 and references therein; Huss et al. 2001; Kunihiro et al. 2004; Bizzarro et al. 2004; Guan et al. 2006; Thrane et al. 2006), some important issues remain unresolved, including the causes of different abundances of ^{26}Al between chondrules, CAIs, AOAs, and among CAIs and chondrules. The former could be attributed to a time difference of formation or a heterogeneous distribution of ^{26}Al in the solar nebula; the latter could be due to formation time difference, heterogeneous distribution of ^{26}Al, or metamorphic redistribution of Mg (e.g., Huss et al. 2001; Rudraswami et al. 2004). Based on high-precision Mg isotope measurements of terrestrial samples, Martian meteorites, and bulk chondrites, Bizzarro et al. (2004) and Thrane et al. (2006) concluded that ^{26}Al was uniformly distributed in the inner solar nebula—the most likely location for the formation of chondrules and refractory inclusions (e.g., Scott and Krot 2005). Metamorphic effects on ^{26}Al-^{26}Mg systematics of chondrules and refractory inclusions can be minimized by studying the most primitive chondrites, such as Semarkona (LL3.0), Bishunpur (LL3.1), Yamato-81020 (CO3.0), and Acfer 094 (ungrouped carbonaceous chondrite). Aluminum-magnesium isotope systematics of chondrules in Yamato-81020, Semarkona, and Bishunpur have been studied in detail (Kita et al. 2000, 2005; McKeegan et al. 2000; Mostefaoui et al. 2002; Yurimoto and Wasson 2000; Kunihiro et al. 2004; Kurahashi et al. 2004; Kurahashi 2006). In spite of the very primitive nature of Acfer 094, Al-Mg systematics of its chondrules and refractory inclusions have not been systematically investigated yet. Hutcheon et al. (2000) reported the presence of ^{26}Mg* (excess in ^{26}Mg due to decay of ^{26}Al) in two Al-rich chondrules from Acfer 094 corresponding to an initial ^{26}Al/^{27}Al ratio of $(1.2 \pm 0.4) \times 10^{-5}$. Here we report ^{26}Al-^{26}Mg systematics of 8 chondrules, 2 AOAs, and 14 CAIs from Acfer 094. The mineralogy and petrography of most of

these objects have been recently described by Krot et al. (2004).

EXPERIMENTAL PROCEDURES

Magnesium isotope compositions of Al-rich and Mg-poor phases (corundum, hibonite, grossite, anorthite, and melilite) in chondrules, AOAs, and CAIs in two polished sections of Acfer 094 were investigated by secondary ion mass spectrometry (SIMS) with a Cameca IMS 6f ion microprobe. An O^- primary beam ~10 μm in diameter was used for sputtering. Positive secondary ions of ^{24}Mg, ^{25}Mg, and ^{26}Mg were collected with an electron multiplier. ^{27}Al was measured with an electron multiplier, or a Faraday cup, if the counting rate was higher than 1.1×10^5 cps. The mass-resolving power was set to ~4000, which is high enough to resolve doubly charged ^{48}Ca from ^{24}Mg. A measurement on one spot took about 1500 seconds. In some spots repeated measurements were made. Magnesium isotope results were expressed as $\Delta^{25}Mg(‰) = ([^{25}Mg/^{24}Mg]_{meas}/0.12663\text{-}1) \times 1000$, and $\Delta^{26}Mg(‰) = ([^{26}Mg/^{24}Mg]_{meas}/0.13932\text{-}1) \times 1000$ (Catanzaro 1966). The excess of ^{26}Mg ($^{26}Mg^*$) was calculated assuming linear mass-dependent fractionation. Relative sensitivity factors for hibonite, grossite, anorthite, pyroxene, olivine, spinel, and melilite were 1.08, 1.08, 1.10, 1.15, 1.15, 1.20, and 1.25, respectively. These are unpublished data for the Cameca IMS 6f at the University of Tokyo except for grossite. The value for grossite was assumed to be the same as that for hibonite based on the similarity in chemical composition (see also Weber et al. 1995). The $^{27}Al^+/^{24}Mg^+$ ionic ratios were divided by the relative sensitivity factor to obtain $^{27}Al/^{24}Mg$ ratios for samples analyzed. 1σ errors of sensitivity factors were estimated to be 5%.

RESULTS

Mineralogy and Petrography

The mineralogy and petrography of most of the refractory inclusions and chondrules analyzed for Mg isotopic compositions in this study were described in detail by Krot et al. (2004). Here we briefly summarize the major characteristics of these objects.

Refractory Inclusions

Sixteen refractory inclusions studied include 14 CAIs and 2 AOAs (Figs. 1 and 2).

CAI s2 is a corundum-rich inclusion with a corundum-hibonite core surrounded by a spinel mantle and a thin Al-diopside rim (Fig. 1a).

CAI #86 is a pyroxene-hibonite spherule composed of an Al-rich (23–44 wt% Al_2O_3) high-Ca pyroxene with several lath-shaped crystals of hibonite, spinel, and melilite (Fig. 1b). Spinel is intergrown with hibonite and appears to replace it. Melilite occurs in the outer portion of the spherule and is extensively corroded by anorthite. The CAI is surrounded by a thin rim of Al-diopside.

CAIs s1, s14, #20, #21, #47, #61, #64, and #68 are grossite-rich/bearing inclusions. Most of them are irregularly shaped objects having a grossite-perovskite ± spinel ± hibonite core surrounded by layers of spinel, melilite, and Al-diopside (Figs. 1 and 2). Occasionally, melilite is replaced by anorthite (Fig. 2d).

CAIs s6, s8, and #95 are melilite-rich inclusions composed of melilite, spinel, perovskite, ±Al,Ti-diopside, and ±hibonite, and surrounded by layers of anorthite and Al-diopside; anorthite replaces melilite (Figs. 2h–j).

CAI #24 is an igneous, anorthite-rich (type C) inclusion composed of anorthite, Al,Ti-diopside, and spinel (Fig. 1d).

AOA #41 is an irregularly shaped object composed of forsterite, anorthite, and Al-diopside (Fig. 2l). Refractory object #11a is mineralogically similar to AOA #41, but has an igneous texture (Fig. 2k), suggesting that it is a melted AOA.

Chondrules

Seven out of eight chondrules studied (numbers 27, 31, 58, 60, 63, 101, and 102) have porphyritic textures and magnesium-rich compositions. These type I chondrules consist of forsteritic olivine and low-Ca pyroxene phenocrysts, Fe,Ni metal nodules, interstitial high-Ca pyroxene and anorthitic plagioclase, and fine-grained mesostasis (Fig. 3). Chondrule #50 is Al-rich; it is composed of pigeonite overgrown by augite, and anorthitic plagioclase (Fig. 4).

Magnesium Isotopic Compositions: The results of Al and Mg isotope measurements in refractory inclusions (CAIs and AOAs), and chondrules from Acfer 094 are summarized in Tables 1 and 2 and illustrated in Figs. 5 and 6. We note that most of the initial $^{26}Al/^{27}Al$ ratios for CAIs were derived from one or two data points. In cases where only one data point was obtained for a CAI, the inferred initial $^{26}Al/^{27}Al$ ratio was calculated assuming a presence of a hypothetical data point with a 2σ error of 2‰ at the origin of the isochron diagram. This is to make the errors of the initial ratios comparable with those that were determined from multiple data points.

Nine of 14 CAIs studied show resolvable $^{26}Mg^*$ in minerals with high (>30) $^{27}Al/^{24}Mg$ ratios (mostly grossite and occasionally melilite). The inferred $^{26}Al/^{27}Al$ ratios in six of them are indistinguishable from the "canonical" ratio of 5.0×10^{-5}. The inferred $^{26}Al/^{27}Al$ ratio in the grossite-rich CAI (s14) (Fig. 2e) is $(6.3 \pm 0.7[2\sigma]) \times 10^{-5}$, considerably higher than the canonical value. The inferred $^{26}Al/^{27}Al$ ratios at the 2σ error limits in CAIs (s6 and #21) are slightly higher than the canonical value. Both AOAs show $^{26}Mg^*$ consistent with the canonical initial $^{26}Al/^{27}Al$ ratio of 5×10^{-5} (Fig. 5a). We note that the initial $^{26}Al/^{27}Al$ ratio is much better defined for

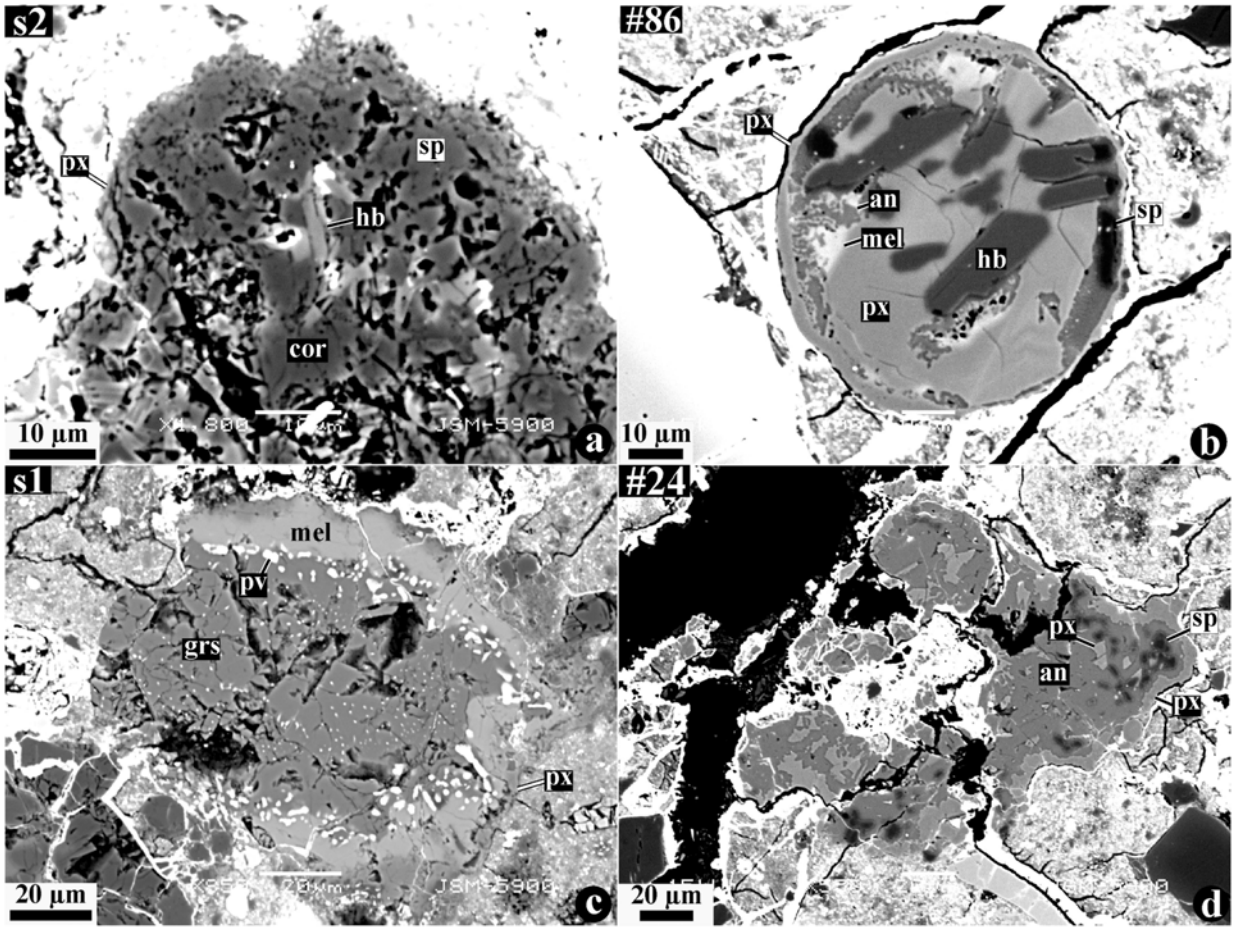

Fig 1. Backscattered electron (BSE) images of the Acfer 0941 CAIs showing no evidence for ^{26}Mg*. a) CAI s2 consists of a corundum-hibonite core surrounded by a spinel mantle and a thin pyroxene rim (outside field of view). b) Pyroxene-hibonite spherule #86 consists of high-Ca pyroxene with highly variable Al_2O_3 content, hibonite, spinel, and melilite that is partly replaced by anorthite; the CAI is surrounded by a rim of Al-diopside. c) Grossite-rich CAI s1 is composed of a grossite-perovskite core surrounded by a melilite mantle and thin Al-diopside rim. d) Igneous, anorthite-rich (type C) CAI #24 is composed of anorthite, Al-diopside, and spinel. an = anorthite; cor = corundum; hb = hibonite; grs = grossite; mel = melilite; px = Al,Ti-diopside; pv = perovskite; sp = spinel.

AOA #11a, having an ^{27}Al/^{24}Mg ratio of ~200 than for AOA #41 (Table 1).

Five CAIs (s1, s2, s8, #86, and #24) show no resolvable ^{26}Mg*. Three of them are very refractory objects composed of corundum, hibonite, grossite, and Al-rich pyroxene (Figs. 1a–c). Hibonite-rich regions of the pyroxene-hibonite spherule #86 analyzed for Mg isotopic compositions have relatively low ^{27}Al/^{24}Mg ratios (20–27). They showed small but resolvable deficits in ^{26}Mg (Table 1; Fig. 5e). Corundum of the CAI s2 and grossite of the CAI s1, with ^{27}Al/^{24}Mg ratio of ~80 and 375–1150, respectively, also show deficits in ^{26}Mg, which, however, within 2σ errors are indistinguishable from 0 (Table 1; Fig. 5d). CAI #24 is an igneous, anorthite-rich type C inclusion (Fig. 1d). Anorthite of CAI #24 with ^{27}Al/^{24}Mg ratio of ~60 has isotopically normal magnesium (Table 1; Fig. 5b). CAI s8 is a melilite-rich inclusion (Fig. 2); its melilite with a low ^{27}Al/^{24}Mg ratio of ~8 has isotopically normal magnesium (Fig. 5b).

The ^{27}Al/^{24}Mg ratios in anorthite in most type I chondrules analyzed range from 20 to 75 with a relatively small spread within each individual chondrule (Table 2). Anorthite in the Al-rich chondrule #50 has a ^{27}Al/^{24}Mg ratio of ~50. The inferred ^{26}Al/^{27}Al ratios differ from 0 at 2σ level in only two chondrules; the inferred ^{26}Al/^{27}Al ratios in these two chondrules are $(10.3 \pm 7.4) \times 10^{-6}$ and $(6.0 \pm 3.8) \times 10^{-6}$, respectively (Table 2; Fig. 6). In comparison, nearly all chondrules studied in Yamato-81020 using a Cameca IMS 1270 ion microprobe show resolvable inferred ^{26}Al/^{27}Al ratios at the 2σ level of ~2×10^{-6} (Kunihiro et al. 2004; Kurahashi et al. 2004; Kurahashi 2006). The lower number of chondrules with resolvable ^{26}Mg* in the present study is due to the larger errors ([3–18] $\times 10^{-6}$ in inferred initial ratios) in our isotopic analyses, which resulted from the low transmission efficiency of the IMS 6f and short measurement times.

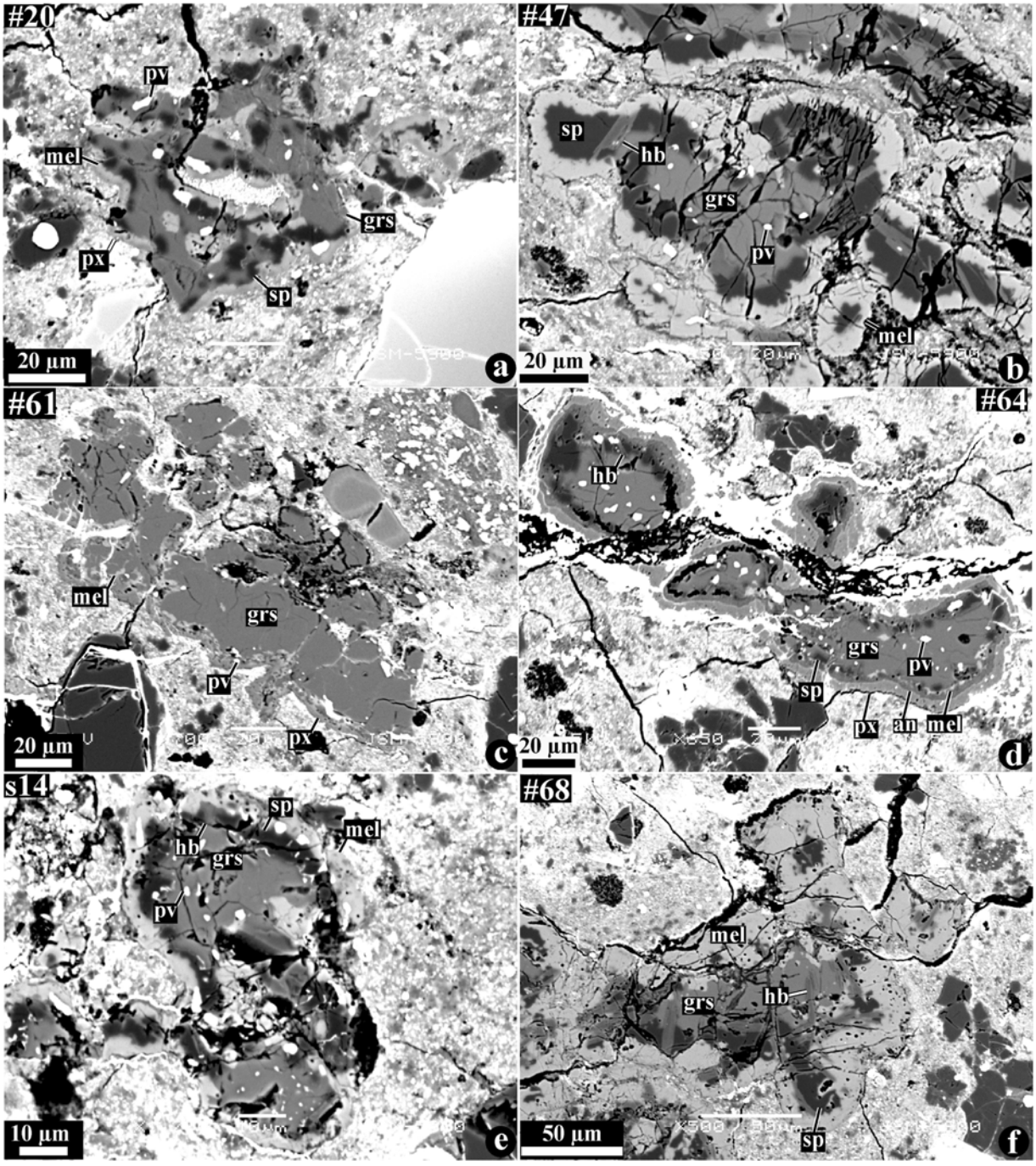

Fig. 2. BSE images of the refractory inclusions showing ^{26}Mg*. a–g) Grossite-rich/bearing CAIs #20, #47, #61, #64, s14, #68, and #21 have a grossite-perovskite ± spinel ± melilite ± hibonite core surrounded by a melilite rim or a melilite-Al-diopside rim. Melilite is occasionally replaced by anorthite. There are significant variations in modal mineralogy of the CAI cores.

DISCUSSION

Based on the measured Mg-isotopic compositions, two groups of refractory inclusions can be recognized in Acfer 094. One group, including 9 CAIs and 2 AOAs, shows ^{26}Mg* corresponding to the canonical ^{26}Al/^{27}Al of 5×10^{-5}; another group composed of 4 CAIs is devoid of ^{26}Mg* (Fig. 5). (The inferred initial ^{26}Al/^{27}Al ratio of CAI s8 has a large error due to a small ^{27}Al/^{24}Mg ratio and cannot be assigned to one of the groups.) Similar bimodal distributions of the ^{26}Al/^{27}Al ratios have been reported in CAIs from other primitive chondrites (e.g., MacPherson et al. 1995; Russell et al. 1998).

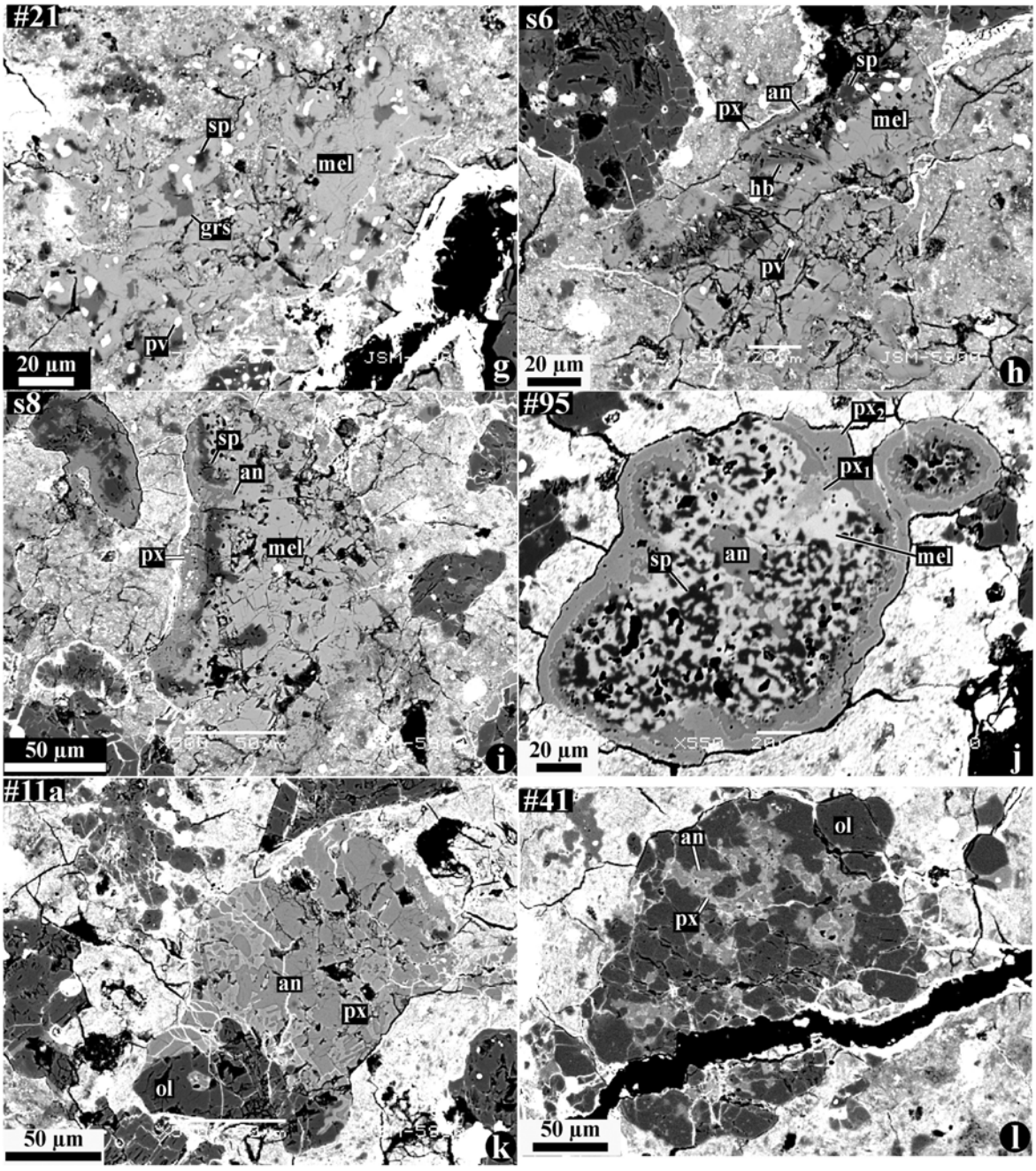

Fig. 2. *Continued.* BSE images of the refractory inclusions showing ^{26}Mg*. h) CAI s6 has a spinel-hibonite core surrounded by a thick melilite mantle and a thin Al-diopside rim. Melilite in the outer part of the inclusion is replaced by anorthite. i) Melilite-rich CAI s8 is surrounded by layers of spinel, anorthite, and Al-diopside. j) Melilite-rich CAI #95 consists of melilite enclosing anhedral spinel grains and minor Al,Ti (px_1); melilite is replaced by anorthite and is surrounded by a rim of diopside (px_2). k) AOA fragment #11a has an igneous texture and consists of anorthite, Al,Ti-diopside, and forsteritic olivine. l) AOA #41 is composed of anorthite, Al,Ti-diopside, and forsteritic olivine. an = anorthite; hb = hibonite; grs = grossite; mel = melilite; px = Al,Ti-diopside; ol = forsteritic olivine; pv = perovskite; sp = spinel.

Anorthite-rich, igneous CAI #24 shows textural evidence for remelting: it lacks Wark-Lovering rim layers, which are observed around most CAIs (e.g., Wark and Lovering 1977; MacPherson 2003 and references therein). As a result, the lack of ^{26}Mg* in CAI #24 could be due to resetting of its Al-Mg system during a late-stage melting event, probably during chondrule formation. Since most CAIs originated in a ^{16}O-rich gaseous reservoir (Krot et al. 2002), whereas most chondrules formed in the presence of ^{16}O-poor nebular gas (e.g., Krot et al., Forthcoming and references therein), this hypothesis can be tested by studying the O-isotopic composition of anorthite in CAI #24. If this CAI was remelted

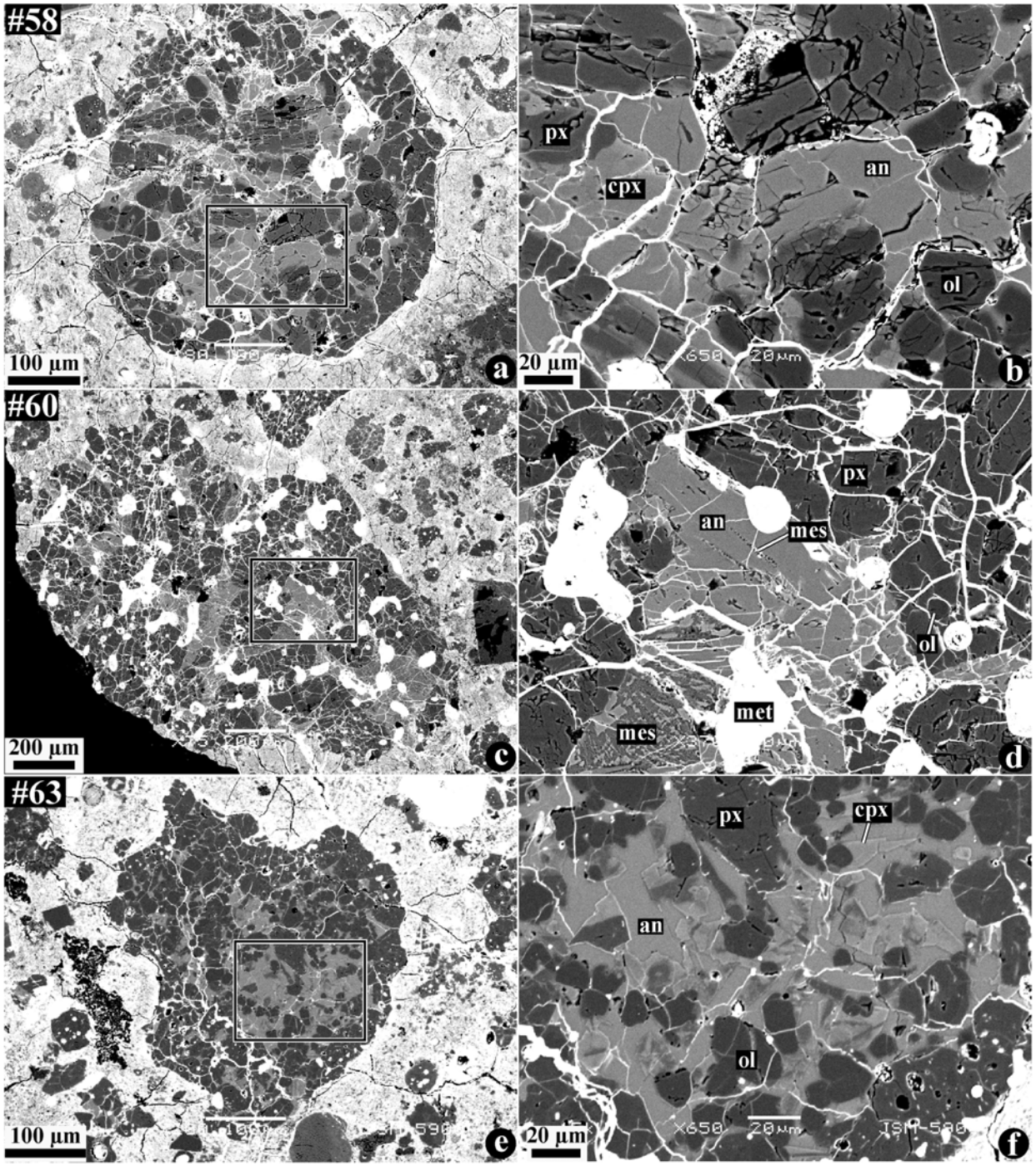

Fig. 3. BSE images of the Acfer 094 magnesium-rich porphyritic (type I) chondrules #58, #60, and #63. The images shown in (b), (d), and (f) are close-up views of the areas in (a), (c), and (e), respectively. an = anorthitic plagioclase; cpx = high-Ca pyroxene; mes = fine-grained mesostasis; met = Fe,Ni metal; ol = forsteritic olivine; px = low-Ca pyroxene.

during the chondrule formation event, it should be ^{16}O-depleted. We note that late-stage remelting of type C CAIs in the chondrule-forming regions accompanied by O-isotopic exchange has been recently reported for the CR (Krot et al. 2005a) and CV (Krot et al. 2005b) carbonaceous chondrites.

The lack of ^{26}Mg* in the other three CAIs, s1, s2, and #86, cannot be attributed to late-stage resetting of the Al-Mg system by remelting, since they either are surrounded by multilayered rims or show deficits in ^{26}Mg* (Fig. 5). We infer that these CAIs contained no ^{26}Al at the time of their formation. All three CAIs are very refractory and composed of

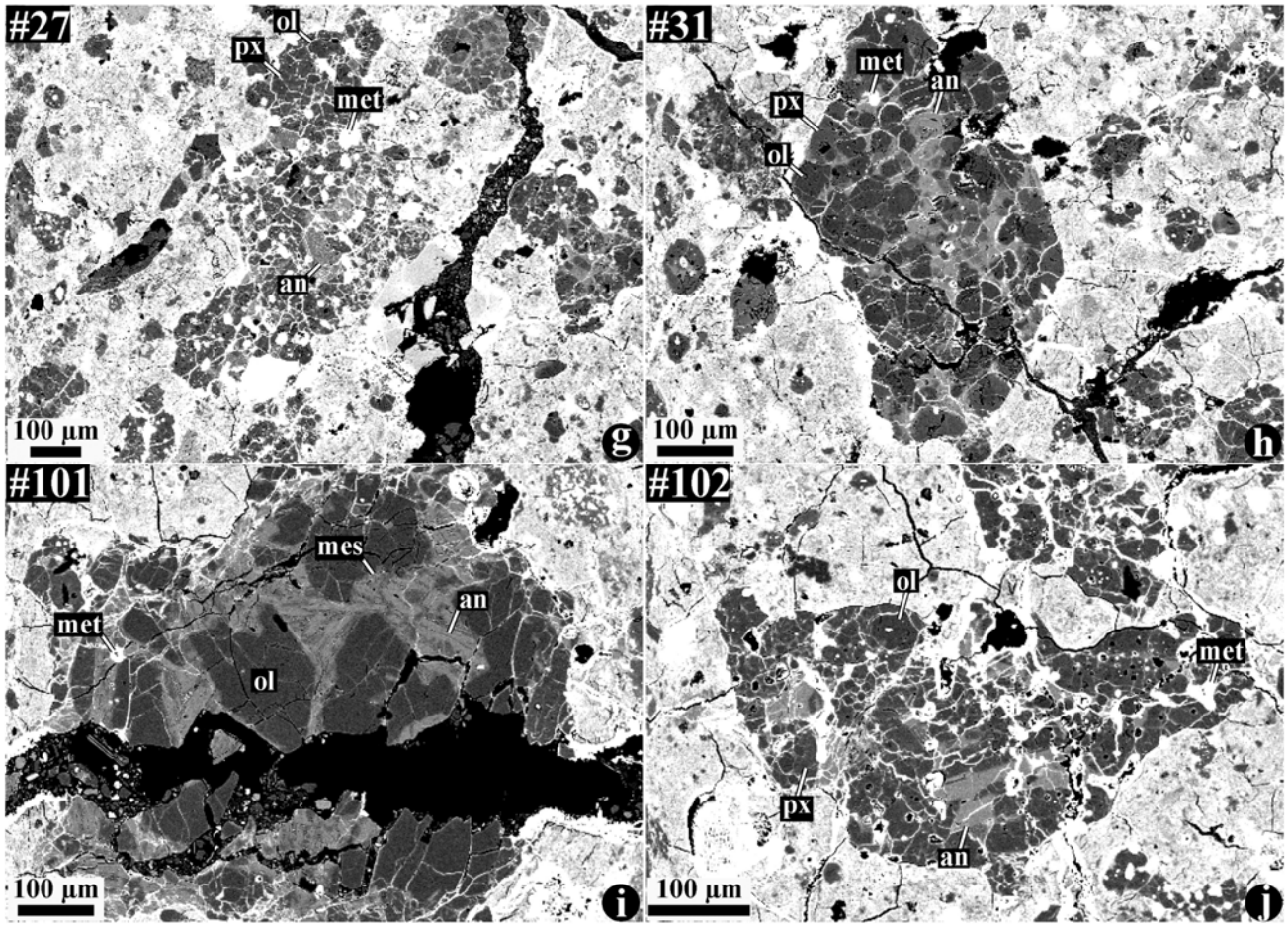

Fig. 3. *Continued.* BSE images of the Acfer 094 magnesium-rich porphyritic (type I) chondrules #27, #31, #101, and #102. an = anorthitic plagioclase; cpx = high-Ca pyroxene; mes = fine-grained mesostasis; met = Fe,Ni metal; ol = forsteritic olivine; px = low-Ca pyroxene.

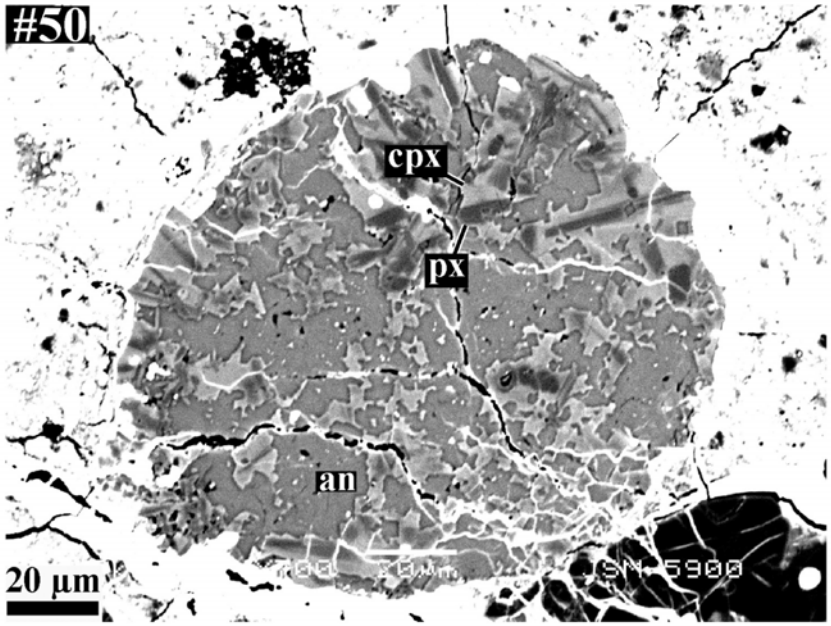

Fig. 4. BSE image of the Acfer 094 aluminum-rich chondrule #50. an = anorthitic plagioclase; cpx = high-Ca pyroxene; px = low-Ca pyroxene.

Table 1. Magnesium isotopic compositions of refractory inclusions from Acfer 094.

Sample	δ^{26}Mg (‰)	2σ (‰)	^{27}Al/^{24}Mg	^{26}Al/^{27}Al (× 10^{-5}) (±2σ)
AOA #11a				5.0 ± 0.7
an	73.6	7.2	204.9	
ol	0.7	1.8	0	
AOA #41				5.7 ± 2.0
an 1	8.5	2.6	15.1	
an 2	6.2	2.5	11.5	
an 3	4.0	2.1	9	
an 4	2.1	2.4	10.1	
an 5	2.7	2.5	12.1	
ol 1	0.0	1.8	0	
ol 2	0.7	1.8	0	
CAI s1				
grs 1	–2.8	4.3	376.4	
grs 2	–6.3	13.4	1148	
CAI s2				
cor 1	–1.3	2.4	70.7	
cor 2	–1	2.5	88.7	
CAI s6				7.1 ± 1.7
mel	18.1	5.2	36.3	
sp	0.7	2.2	2	
CAI s8				3.5 ± 4.9[a]
mel	2.0	2.1	8	
CAI s14				6.3 ± 0.7[a]
grs	185	9.7	408	
CAI #20				5.9 ± 1.1[a]
grs + mel	20	4.4	41.8	
grs + mel	27	5.5	68.3	
CAI #21				7.6 ± 2.5[a]
mel	27	8.3	49.2	
CAI #24				–0.2 ± 1.3[a]
an 1	2	7.9	60.7	
an 2	–3.6	7.7	60.4	
CAI #47				4.7 ± 0.5[a]
grs	40.2	8.0	119.3	
CAI #61				5.0 ± 1.1[a]
grs	131	14.3	367	
CAI #64				5.2 ± 0.6[a]
grs	475	29	1267	
CAI #68				4.6 ± 1.5
grs 1	26.7	11.0	70.3	
grs 2	44.6	17.6	150.1	
grs 3	35	17.1	81.6	
sp	0.5	2.3	3	
CAI #86				
px 1	–1.2	2.9	4.6	
px 2	–1.2	2.6	4.7	
px 3	0.3	2.6	4.7	
px 4	–2	2.1	21.8	
px 5	–1.6	2.1	21.3	
hib + px 1	–4.3	3.5	27.3	
hib + px 2	–3.8	3.4	26.2	
hib + px 3	–2.4	2.1	20.5	
hib + px 4	–3.3	2.1	20.1	
CAI #95				5.1 ± 0.8
an	107	13.6	297	
di	–1.7	1.8	0	

[a]Forced to pass through origin.

corundum, grossite, hibonite, and Al-rich pyroxene. Mineralogically similar CAIs with no ^{26}Mg* have been previously described in primitive (CM2, CH3.0, and CO3.0) carbonaceous chondrites (e.g., Ireland et al. 1991; Weber et al. 1995; Russell et al. 1998; Simon et al. 2002; Liu et al. 2006). Some of these CAIs show significant isotopic fractionations and/or isotope anomalies in Ca and Ti that are due to unknown nuclear effects, and are called FUN inclusions. A subset of FUN without large isotopic fractionations are called UN inclusions. The lack of ^{26}Mg* in these inclusions has been attributed either to their formation prior to the injection of ^{26}Al into the protoplanetary disk or to local heterogeneity in the ^{26}Al distribution (e.g., Weber et al. 1995; Sahijpal and Goswami 1998). CAIs s1, s2, and #86 may belong to the group of UN inclusions, because we have not detected large Mg isotope fractionation in these samples. Fractionation of ^{25}Mg relative to the reference value (Catanzaro et al. 1966) is several ‰ negative in s1 and #86, and several ‰ positive in s2. (Under the measurement condition, the instrumental fractionation was not well controlled and therefore these fractionations were probably mainly due to instrumental effects.) We note that Ca and Ti isotopic compositions have not been measured yet. The magnitude of the ^{26}Mg deficit in hibonite + Al-rich pyroxene of #86 is similar to the largest deficit previously reported for hibonite from Murchison. A deficit in ^{26}Mg of –4.74 ± 2.28‰ was reported for a platy hibonite (Ireland 1988) and 4‰ deficit was reported for a hibonite spherule (Liu et al. 2006). There seems to be a negative correlation between the Al/Mg ratio and the ^{26}Mg* in this CAI (Fig. 5e). The Mg-rich rim (spots px1, px2, and px3 with low Al/Mg ratios in Table 1) of Al-diopside around #86 shows smaller anomalies compared with the Mg-poor interior, which may have resulted from mixing between an anomalous interior component and a more normal component condensing onto the rim from the nebula gas. CAIs s1 and s2 also show small negative ^{26}Mg anomalies, although each datum is mostly insignificant within 1σ error. Since the CAIs measured by SIMS in this study were chosen randomly (mainly based on the presence of Al-rich phases more than 10 μm in diameter), the fraction (~20%) of CAIs with Al-rich phases in this chondrite that formed without ^{26}Al may be considered as a relatively unbiased value. We note that CAIs mainly

Table 2. Magnesium isotopic compositions of chondrules from Acfer 094.

Sample	δ^{26}Mg (‰)	2σ (‰)	^{27}Al/^{24}Mg	^{26}Al/^{27}Al (× 10^{-6}) (±2σ)
chd #27				2.4 ± 9.4
an 1	–0.1	2.2	29.1	
an 2	0.2	2.3	30.7	
an 3	1.9	2.0	20.1	
an 4	2.5	2.0	19.7	
px 1	1.4	1.9	0	
px 2	–0.9	1.9	0	
chd #31				10.3 ± 7.4
an 1	2.7	2.0	24.9	
an 2	1.5	2.0	24.3	
an 3	–0.6	2.3	27.8	
an 4	2.4	2.9	23	
an 5	2.2	2.9	26.7	
an 6	1.4	3.4	29.6	
an 7	–0.3	3.2	27.8	
ol 1	0.1	1.9	0	
ol 2	–0.6	1.9	0	
ol 3	–1.0	2.0	0	
ol 4	–0.8	2.1	0	
chd #50				–0.1 ± 6.7
an 1	–0.7	3.6	52.3	
an 2	–1.5	3.4	43.9	
an 3	1.0	2.6	24.1	
an 4	–2.0	2.6	23.8	
an 5	6.1	6.0	53.5	
an 6	0.8	5.9	50	
di -1	0.1	2.1	0.1	
di -2	–0.3	2.1	0.1	
di -3	0.3	2.1	0.1	
chd #58				3.1 ± 5.8
an 1	2.3	2.4	34.5	
an 2	0.2	2.3	34.9	
an 3	1.1	2.4	39.1	
an 4	1.9	2.4	38.6	
px 1	1.4	2.0	0	
px 2	–0.1	1.9	0	
px 3	–0.4	1.9	0	
px 4	1.3	1.9	0	
chd #60				6.0 ± 3.8
an 1	1.8	1.8	25.3	
an 2	1.6	2.0	34.6	
an 3	2.0	1.8	39	
an 4	2.6	2.0	39.4	
an 5	1.3	2.1	35.1	
an 6	1.1	2.1	36	
an 7	0.3	2.0	35.9	
an 8	2.3	2.0	33.1	
an 9	1.3	2.0	32.6	
an 10	0.0	2.3	39.7	
an 11	2.2	2.3	39.6	
an 12	0.8	2.0	29.9	
px 1	–1.3	1.8	0	
px 2	–0.2	1.7	0	
px 3	0.8	2.0	0	
px 4	0.5	2.0	0	
px 5	–0.9	1.9	0	
px 6	0.9	1.9	0	
chd #63				4.9 ± 17.9
an 1	0.8	6.8	31.9	
an 2	4.5	7.1	32.7	
an 3	–5.4	6.9	32.1	
ol 1	–1.0	1.9	0	
ol 2	–2.7	1.9	0	
ol 3	0.2	1.9	0	
chd #101				1.7 ± 4.4
an 1	1.3	2.2	61.8	
an 2	0.7	2.8	63.3	
an 3	0.4	5.4	74.5	
ol	0.2	1.2	0	
chd #102				5.9 ± 10.1
an 1	1.7	4.2	32.8	
an 2	3.5	4.2	32.3	
an 3	–1.7	4.2	31.8	
an 4	1.0	3.9	31.7	
px 1	0.0	1.9	0	
px 2	–0.8	2.0	0	
px 3	0.1	2.0	0	

consisting of spinel and pyroxene were not included in this study due to lack of Al-rich phases. Therefore, 20% is a slight overestimate for the whole population of CAIs.

The other CAIs and AOAs show nearly canonical values of inferred initial ^{26}Al/^{27}Al ratios. Among phases with high ^{27}Al/^{24}Mg ratio, grossite in CAI s14 shows the highest inferred initial ^{26}Al/^{27}Al ratio of $(6.3 \pm 0.7) \times 10^{-5}$ at the 2σ error limit. Although the sensitivity factor for grossite is not well known, this initial ratio is significantly higher than those for grossites in other CAIs (e.g., #64). Therefore, the high inferred initial ratio is not due to an inappropriate choice of the sensitivity factor. If one uses the nominal errors for the inferred initial ratios given in Table 1, the initial ^{26}Al/^{27}Al ratios for s14 and #64 are not significantly different at the 2σ level. However, the errors given in Table 1 for the inferred initial ratios are mainly due to uncertainties of the relative sensitivity factor. Errors due to counting statistics are about 6% (2σ) of the signal for both s14 and #64. When comparing the data among grossites, errors due to the relative sensitivity factor can be practically ignored compared with the 6% errors. Using only the latter, the ^{26}Al/^{27}Al initial ratios for s14 $(6.3 \pm 0.4) \times 10^{-5}$ and #64 $(5.2 \pm 0.3) \times 10^{-5}$ are significantly different at the 2σ level. The observed range of the inferred initial ^{26}Al/^{27}Al ratios from $\sim 5 \times 10^{-5}$ to 6.3×10^{-5} in the Acfer 094 CAIs appears to be consistent with those from the Allende CAIs reported by Young et al. (2005) and Taylor

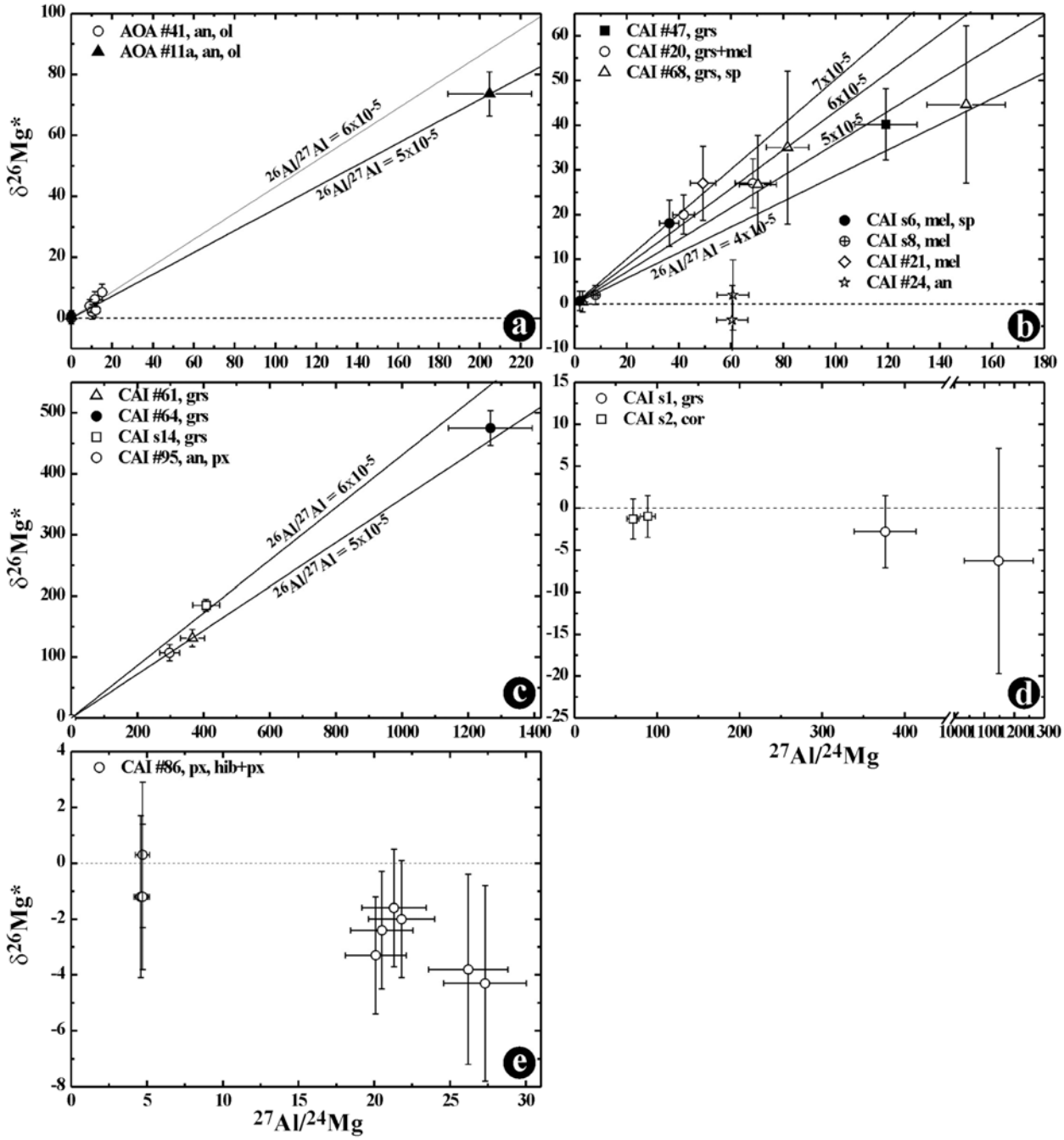

Fig. 5. Aluminum-magnesium isochron diagrams of the Acfer 094 AOAs (a) and CAIs (b–e). The error bars attached to the data points are 2σ. $^{26}Al/^{27}Al$ ratios between 4×10^{-5} and 7×10^{-5} in (a), (b), and (c) are shown for reference. Minerals analyzed are listed in the legends. an = anorthite; cor = corundum; grs = grossite; hib = hibonite; mel = melilite; px = Al,Ti-diopside; ol = forsteritic olivine; sp = spinel.

et al. (2005) and may indicate that CAI formation continued for ~300,000 years.

Intermediate inferred initial $^{26}Al/^{27}Al$ ratios between 1×10^{-5} and 4×10^{-5}, resulting from later disturbance, are often reported in literature (MacPherson et al. 1995, and references therein). Such data are absent in this study. Since Acfer 094 is one of the most primitive (unaltered and unmetamorphosed) chondrites, this may suggest that the intermediate values resulted from partial resetting of Al-Mg systematics during thermal metamorphism. We note, however, that none of the Acfer 094 CAIs studied belong to a type B type for which the intermediate values are most often reported.

Both AOAs (#41 and #11a) show $^{26}Mg^*$ consistent with the canonical $^{26}Al/^{27}Al$ ratio (Fig. 5a), suggesting contemporaneous formation with CAIs (Figs. 5b and 5c). This is in contrast to the inferred initial ratios of $(2.7 \pm 0.7) \times$

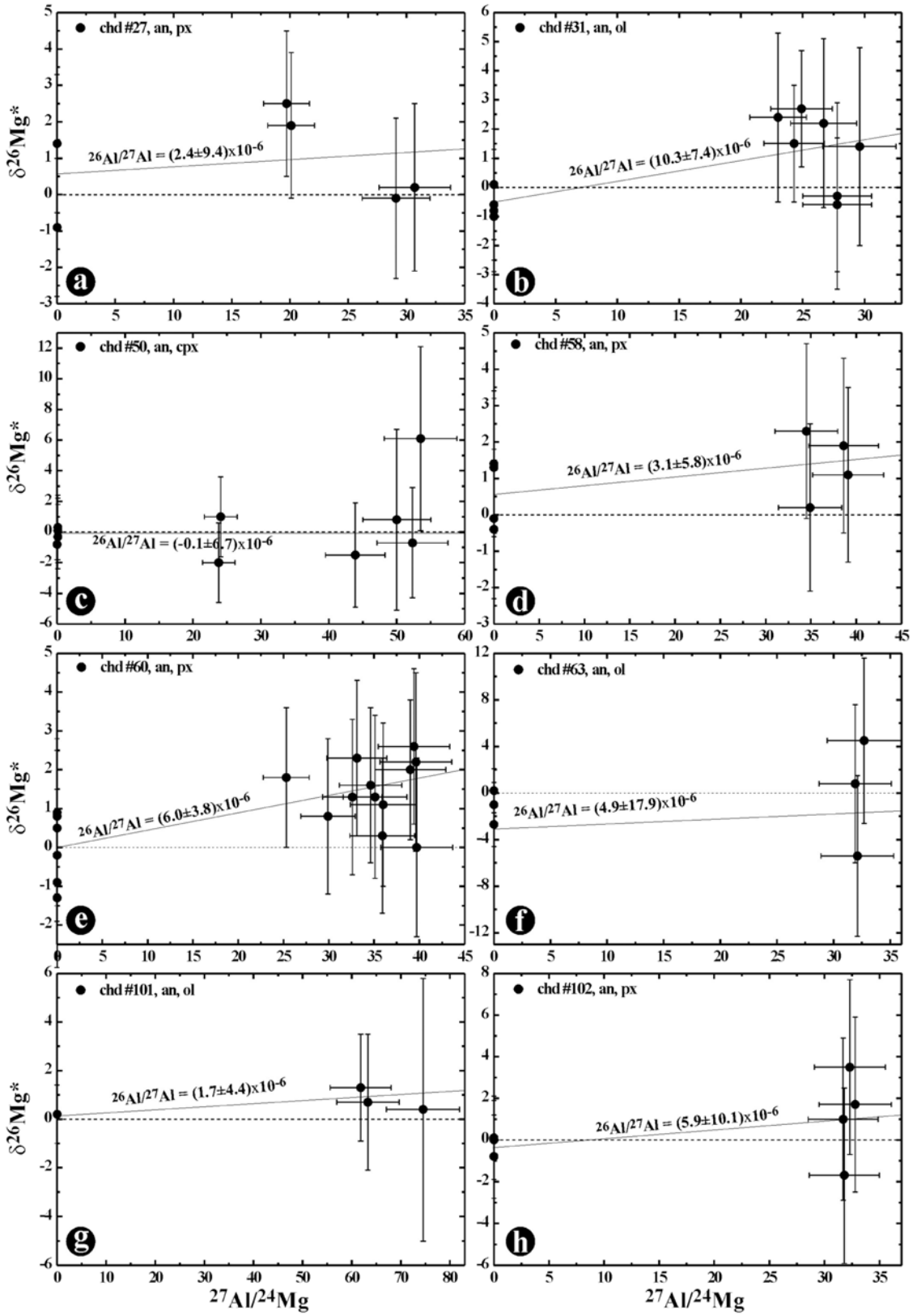

Fig. 6. Aluminum-magnesium isochron diagrams of the Acfer 094 chondrules. Minerals analyzed are listed in the legends. The error bars attached to the data points are 2σ. Errors attached to the inferred initial ^{26}Al/^{27}Al ratios are 2σ. an = anorthitic plagioclase; cpx = high-Ca pyroxene; px = low-Ca pyroxene; ol = forsteritic olivine.

10^{-5}, $(2.9 \pm 1.5) \times 10^{-5}$, and $(3.2 \pm 1.5) \times 10^{-5}$ in three AOAs from Yamato-81020 (Itoh et al. 2002). A slight difference in the degrees of thermal metamorphism experienced by Acfer 094 and Yamato-81020 or differences in the sizes of the measured grains may explain the different inferred initial ratios between these two chondrites. Based on the Cr contents in olivine of type II chondrules, Grossman and Brearley (2005) concluded that Acfer 094 is slightly less metamorphosed than Yamato-81020. The measured spot sizes in Acfer 094 of this study are about ~10 μm in diameter in large anorthite grains (Figs. 2k and 2l), whereas those measured by Itoh et al. (2002) are ~2–5 μm in diameter in presumably smaller grains, although a full description of the anorthite grain size was not provided. Smaller grains could be disturbed more easily than larger grains. Therefore, both interpretations are viable at present. Examination of large anorthite grains in Yamato-81020 should provide a test of the latter hypothesis.

If a chronological interpretation of the inferred initial $^{26}Al/^{27}Al$ ratios of chondrules is adopted, the formation ages relative to CAIs of chondrule #31 and chondrule #60 are $1.6^{+1.2}_{-0.6}$ Myr and $2.2^{+0.4}_{-0.3}$ Myr, respectively. These ages are similar to those reported for type I chondrules in Yamato-81020 (Kurahashi et al. 2004). These ages are also similar to the chondrule ages in the primitive ordinary chondrites Semarkona and Bishunpur (Kita et al. 2000; McKeegan et al. 2000; Mostefaoui et al. 2002). The similarity of chondrule ages in Acfer 094, Yamato-81020, Semarkona, and Bishunpur suggests that metamorphism did not affect chondrule ages in these meteorites, contrary to ordinary chondrite chondrules of higher petrologic types (equal to or higher than type 3.5; Huss et al. 2001).

CONCLUSIONS

We reported in situ magnesium isotope measurements of 7 type I chondrules, 1 Al-rich chondrule, 14 CAIs, and 2 AOAs from the ungrouped carbonaceous chondrite Acfer 094 using a Cameca-6f ion microprobe.

About 20% of the Acfer 094 CAIs studied appear to have formed without ^{26}Al. Most CAIs show inferred initial $^{26}Al/^{27}Al$ ratios within error in agreement with the canonical ratio of 5×10^{-5}. An inferred initial $^{26}Al/^{27}Al$ ratio in one of the grossite-rich CAIs is 6.3×10^{-5}. We infer that formation of CAIs from Acfer 094 may have lasted for ~300,000 years. The lack of CAIs with intermediate $^{26}Al/^{27}Al$ ratios may indicate that at least some of the intermediate values reported in the literature resulted from partial resetting of the ^{26}Al-^{26}Mg system during thermal metamorphism. Two AOAs show $^{26}Mg^*$ corresponding to the $^{26}Al/^{27}Al$ ratio of $\sim 5 \times 10^{-5}$, suggesting contemporaneous formation with CAIs.

The inferred initial $^{26}Al/^{27}Al$ ratios in two type I chondrules from Acfer 094 ($[10.3 \pm 7.4] \times 10^{-6}$ and $[6.0 \pm 3.8] \times 10^{-6}$) are similar to those previously reported in type I chondrules from Yamato-81020 (CO3.0), Semarkona (LL3.0), and Bishunpur (LL3.1), suggesting that metamorphism has not affected the Al-Mg system of chondrules in these meteorites. The inferred $^{26}Al/^{27}Al$ ratios in the Acfer 094 chondrules correspond to age differences of $1.6^{+1.2}_{-0.6}$ and $2.2^{+0.4}_{-0.3}$ Myr relative to CAIs with the canonical $^{26}Al/^{27}Al$ ratio.

Acknowledgments–We wish to thank Dr. A. Miyazaki for assistance with SIMS measurements and Dr. H. Hiyagon for discussion. We thank Drs. E. Zinner, M. Trielof, and an anonymous reviewer for constructive comments.

Editorial Handling—Dr. Larry Nittler

REFERENCES

Bizzarro M., Baker J. A., and Haack H. 2004. Mg isotope evidence for contemporaneous formation of chondrules and refractory inclusions. *Nature* 431:275–278.

Catanzaro E. J., Murphy T. J., Garner E. L., and Shields W. R. 1966. Absolute isotopic abundance ratios and atomic weights of magnesium. *Journal of Research of the National Bureau of Standards* 70A:453–458.

Grossman J. N. and Brearley A. J. 2005. The onset of metamorphism in ordinary and carbonaceous chondrites. *Meteoritics & Planetary Science* 40:87–122.

Guan Y., Huss G. R., Leshin L. A., MacPherson G. J., and McKeegan K. D. 2006. Oxygen isotope and ^{26}Al-^{26}Mg systematics of aluminum-rich chondrules from unequilibrated enstatite chondrites. *Meteoritics & Planetary Science* 41:33–47.

Huss G. R., MacPherson G. L., Wasserburg G. J., Russell S. S., and Srinivasan G. 2001. Aluminum-26 in calcium-aluminum-rich inclusions and chondrules from unequilibrated ordinary chondrites. *Meteoritics & Planetary Science* 36:975–997.

Hutcheon I. D., Krot A. N., and Ulyanov A. A. 2000. ^{26}Al in anorthite-rich chondrules in primitive carbonaceous chondrites: Evidence chondrules post-date CAI (abstract #1869). 31st Lunar and Planetary Science Conference. CD-ROM.

Ireland T. R. 1988. Correlated morphological, chemical, and isotopic characteristics of hibonites from the Murchison carbonaceous chondrite. *Geochimica et Cosmochimica Acta* 52:2827–2839.

Ireland T. R., Fahey A. J., and Zinner E. 1991. Hibonite-bearing microspherules—A new type of refractory inclusions with large isotopic anomalies. *Geochimica et Cosmochimica Acta* 55:367–379.

Itoh S., Rubin A. E., Kojima H., Wasson J. T., and Yurimoto H. 2002. Amoeboid olivine aggregates and AOA-bearing chondrule from Y-81020 CO3.0 chondrite: Distributions of oxygen and magnesium isotopes (abstract #1490). 33rd Lunar and Planetary Science Conference. CD-ROM.

Kita N. T., Nagahara H., Togashi S., and Morishita Y. 2000. A short duration of chondrule formation in the solar nebula: Evidence from ^{26}Al in Semarkona ferromagnesian chondrules. *Geochimica et Cosmochimica Acta* 64:3913–3922.

Kita N. T., Tomomura S., Tachibana S., Nagahara H., Mostefaoui S., and Morishita Y. 2005. Correlation between aluminum-26 ages and bulk Si/Mg ratios for chondrules from LL3.0–3.1 chondrites (abstract #1750). 37th Lunar and Planetary Science Conference. CD-ROM.

Krot A. N., McKeegan K. D., Leshin L. A., MacPherson G. J., and

Scott E. R. D. 2002. Existence of an ^{16}O-rich gaseous reservoir in the solar nebula. *Science* 295:1051–1054.

Krot A. N., Fagan T. I., Keil K., McKeegan K. D., Sahijpal S., Hutcheon I. D., Petaev M. I., and Yurimoto H. 2004. Ca,Al-rich inclusions, amoeboid olivine aggregates, and Al-rich chondrules from the unique carbonaceous chondrite Acfer 094: I. Mineralogy and petrology. *Geochimica et Cosmochimica Acta* 68:2167–2184.

Krot A. N., Hutcheon I. D., Yurimoto H., Cuzzi J. N., McKeegan K. D., Scott E. R. D., Libourel G., Chaussidon M., Aléon J., and Petaev M. I. 2005a. Evolution of oxygen isotopic composition in the inner solar nebula. *The Astrophysical Journal* 622:1333–1342.

Krot A. N., Yurimoto H., Hutcheon I. D., and MacPherson G. J. 2005b. Relative chronology of CAI and chondrule formation: Evidence from chondrule-bearing igneous CAIs. *Nature* 434: 998–1001.

Krot A. N., Yurimoto H., McKeegan K. D., Leshin L., Chaussidon M., Libourel G., Yoshitake M., Huss G. R., Guan Y., and Zanda B. Forthcoming. Oxygen isotopic compositions of chondrules: Implication for understanding oxygen isotope evolution of the solar nebula. *Chemie der Erde.*

Kunihiro T., Rubin A. E., McKeegan K. D., and Wasson J. T. 2004. Initial ^{26}Al/^{27}Al in carbonaceous-chondrite chondrules: Too little ^{26}Al to melt asteroids. *Geochimica et Cosmochimica Acta* 68: 2947–2957.

Kurahashi E., Kita N. T., Nagahara H., and Morishita Y. 2004. Contemporaneous chondrule formation between ordinary and carbonaceous chondrites (abstract #1476). 35th Lunar and Planetary Science Conference. CD-ROM.

Kurahashi E. 2006. Evolution of solid materials in the protoplanetary disk: Constraints from ^{26}Al ages and cosmochemical properties of chondrules in a primitive CO chondrite. Ph.D. thesis, University of Tokyo, Tokyo, Japan.

Lee T., Papanastassiou D. A., and Wasserburg G. J. 1976. Demonstration of ^{26}Mg excess in Allende and evidence for ^{26}Al. *Geophysical Research Letters* 3:41–44.

Liu M.-C., McKeegan K. D., and Davis A. M. 2006. Magnesium isotopic compositions of CM hibonite grains (abstract #2428). 37th Lunar and Planetary Science Conference. CD-ROM.

MacPherson G. J., Davis A. M., and Zinner E. K. 1995. The distribution of aluminum-26 in the early solar system. *Meteoritics* 30:365–386.

MacPherson G. J. 2003. Calcium-aluminum-rich inclusions in chondritic meteorites. In *Meteorites, comets, and planets*, edited by Davis A. M. Treatise on Geochemistry, vol. 1. Oxford: Elsevier. pp. 201–247.

McKeegan K. D., Greenwood J. P., Leshin L. A., and Cosarinsky M. 2000. Abundance of ^{26}Al in ferromagnesian chondrules of unequilibrated ordinary chondrites (abstract #2009). 31st Lunar and Planetary Science Conference. CD-ROM.

Mostefaoui S., Kita N. T., Togashi S., Tachibana S., Nagahara H., and Morishita Y. 2002. The relative formation ages of ferromagnesian chondrules inferred from their initial aluminum-26/aluminum-27 ratios. *Meteoritics & Planetary Science* 37: 421–438.

Rudraswami N. G., Deomurari M. P., and Goswami J. N. 2004. Al-Mg isotope systematics in ferromagnesian chondrules from the unequilibrated ordinary chondrite Adrar 003: Time scale of chondrule formation (abstract #1236). 35th Lunar and Planetary Science Conference. CD-ROM.

Russell S. S., Huss G. R., Fahey A. J., Greenwood R. C., Hutchison R., and Wasserburg G. J. 1998. An isotopic and petrologic study of calcium-aluminum-rich inclusions from CO3 chondrites. *Geochimica et Cosmochimica Acta* 62:689–714.

Sahijpal S. and Goswami J. N. 1998. Refractory phases in primitive meteorites devoid of ^{26}Al and ^{41}Ca: Representative samples of first solar system solids? *The Astrophysical Journal* 509:L137–L140.

Scott E. R. D. and Krot A. N. 2005. Chondritic meteorites and the high-temperature nebular origins of their components. In *Chondrites and the protoplanetary disk*, edited by Krot A. N., Scott E. R. D., and Reipurth B. San Francisco: Astronomical Society of the Pacific. pp. 15–54.

Simon S. B., Davis A. M., Grossman L., and McKeegan K. D. 2002. A hibonite-corundum inclusion from Murchison: A first-generation condensate from the solar nebula. *Meteoritics & Planetary Science* 37:533–548.

Taylor D. J., Cosarinsky M., Liu M.-C., McKeegan K. D., Krot A. N., and Hutcheon I. D. 2005. Survey of initial ^{26}Al in type A and B CAIs: Evidence for an extended formation period for refractory inclusions (abstract). *Meteoritics & Planetary Science* 40:A151.

Thrane K., Bizzarro M., and Baker J. A. 2006. Extremely brief formation interval for refractory inclusions and uniform distribution of ^{26}Al in the early solar system. *The Astrophysical Journal* 646:L159–L162.

Wark D. A. and Lovering J. F. 1977. Marker events in the early evolution of the solar system: Evidence from rims on Ca-Al-rich inclusions in carbonaceous chondrites. Proceedings, 8th Lunar Science Conference. pp. 85–112.

Weber D., Zinner E., and Bischoff A. 1995. Trace element abundances and magnesium, calcium, and titanium isotopic compositions of grossite-containing inclusions from the carbonaceous chondrite Acfer 182. *Geochimica et Cosmochimica Acta* 59:803–823.

Young E. D., Simon J. I., Galy A., Russell S. S., Tonui E., and Lovera O. 2005. Supra-canonical ^{26}Al/^{27}Al and the residence time of CAIs in the solar protoplanetary disk. *Science* 308:223–227.

Yurimoto H. and Wasson J. T. 2002. Extremely rapid cooling of a carbonaceous-chondrite chondrule containing very ^{16}O-rich olivine and a ^{26}Mg-excess. *Geochimica et Cosmochimica Acta* 66:4355–4363.